Effect of nonzero chain diameter on ''DNA'' condensation

B.-Y. Ha[1] and Andrea J. Liu[2]
[1]Department of Physics, Simon Fraser University, Burnaby, British Columbia V5 156, Canada
[2]Department of Chemistry and Biochemistry, University of California, Los Angeles, California 90095
(Received 22 November 1999; published 22 January 2001)

We present a simple model to investigate the effect of chain diameter on multivalent-counterion-induced attractions between two charged chains. In our minimal model, the chains are rigid rods of diameter D with a uniform charge density on the surface, and the counterions are point ions. As a function of the separation between two rods, we find a repulsive barrier in the free energy whose height increases with D. We have also explored the effect of counterion valency Z on the interaction. For parameters characteristic of DNA, we find that a minimum valency of $Z=3$ is required to produce condensation. We also find that the shape of the potential is fairly insensitive to Z for $Z \geqslant 3$. These results are consistent with experimental observations of DNA condensation.

DOI: 10.1103/PhysRevE.63.021503 PACS number(s): 61.25.Hq, 61.20.Qg, 87.15.Nn

I. INTRODUCTION

Polymer physicists typically treat polymers as infinitely thin objects. Microscopic details such as monomer size and shape are usually subsumed into a single parameter, the persistence length, because they do not otherwise affect large-length-scale properties. Even for polyelectrolytes in solution with counterions, it has proven useful to model the polyelectrolyte chains as line charges. This simplification has proven to be particularly useful at high temperatures or for weakly charged polyelectrolytes [1].

Here we show that the approximation of treating a polyelectrolyte as a line charge can lead to gross quantitative errors in treating DNA condensation. This electrostatic phenomenon occurs when salts with multivalent cations are added to DNA solution [2] and the chains self-assemble into concentrated bundles. DNA chains are highly negatively charged in aqueous solution. Some fraction of the cations stay near the chain; these are known as condensed counterions, and they are distributed nonuniformly along the lengths of the chains. Charge distributions on different chains can become correlated when the chains are close together; this leads to the attraction responsible for drawing the DNA chains together into concentrated bundles. There is also a repulsion between chains, which arises because not all of the backbone charge is neutralized by condensed counterions, so the chains still carry a net negative charge.

The balance of the attractive and repulsive interactions depends sensitively on the radius of the chain, especially when the charge is at the surface of the chain (as is the case with DNA). In our approach, the counterions are divided into two classes, free and condensed, and the chains are modeled as cylinders of diameter D. Within our approximation, condensed counterions merely modify the local charge at the surface of a cylinder, giving rise to charge fluctuations on the two-dimensional surface of each cylinder.

Lau and Pincus [3] recently used a similar model, in the special case of zero net charge and no added salt, to study how charge fluctuations affect the bending rigidity of a membrane. The problem we consider here is more complicated because we consider the interaction between two parallel cylinders, and because we treat the case of nonzero net charge, where there is a repulsion between the cylinders as well as a correlation attraction.

II. MODEL AND CALCULATION

In order to treat two-dimensional charge fluctuations on the surface of a cylindrical rod, we define each monomer to be a circular ring of N sites, where each site has length and width b that can carry charges. The cylindrical rod is a stack of M such monomers. Thus, the length of the cylinder is Mb, the circumference of the cylinder is Nb, and there are MN sites on the cylinder that can carry a charge. Each site carries base negative backbone charge of $-e/N$, so that the total charge per monomer is $-e$. In addition, the charge of a site can be modified if there is a counterion present. We allow for two kinds of cations, monovalent cations and multivalent cations of valence Z. Both valencies of cations are subdivided into two classes, condensed and free. The average number of condensed monovalent cations per site is denoted as f_1/N and the average number of condensed multivalent cations (with the valency Z) per site is denoted as f_2/N. Because the condensed cations are assumed to modify the local charge, the dimensionless charge on site j of monomer s (in units of electronic charge e) is a fluctuating variable and can assume the values

$$q_j(s) = -1/N + m_1 + m_2 Z, \tag{1}$$

where $m_1, m_2 = 0,1,2,\ldots,$ are the numbers of condensed monovalent and multivalent cations, respectively, that are closest to the site. The random variables m_1 and m_2 then satisfy $\langle m_i \rangle = f_i/N$.

Note that all sites on the surface of a cylindrical rod are equivalent in our model. We have neglected the fact that the negative charges are localized on phosphate groups at specific sites on double-stranded DNA, and that positive ions may also tend to be localized at specific sites along the helix. Inclusion of these effects at *zero temperature* leads to additional attractions [4]. We are interested in studying the phenomenon at nonzero temperatures. It is possible to include

the localization of charge at specific sites in our formulation, but that makes the calculation remarkably tedious and does not contribute much new insight into the nature of the interactions.

For a given charge configuration in our model, the electrostatic energy is simply given by the unscreened Coulomb interactions between all charges in the system, including the mobile ions. To evaluate the free energy, we first integrate over the mobile ions at the Gaussian level [5]. This is equivalent to treating the mobile ions with the Debye-Hückel approximation [1]. The next step is to integrate over the charge fluctuations on each cylinder surface. For the purposes of the calculation, it is more convenient to describe the cylinder as a circular array of N slabs that are one site thick and M sites long, instead of as a stack of M rings that are N sites in circumference and one site long. We then make the continuum approximation along the length of the slabs. The resulting free energy can be expressed in terms of the following block matrices:

$$ {}^0\boldsymbol{Q}=\begin{pmatrix} {}^0Q_{I\,I} & {}^0Q_{I\,II} \\ {}^0Q_{II\,I} & {}^0Q_{II\,II} \end{pmatrix}, \quad \boldsymbol{Q}(k)=\begin{pmatrix} Q_{I\,I}(k) & Q_{I\,II}(k) \\ Q_{II\,I}(k) & Q_{II\,II}(k) \end{pmatrix} \tag{2} $$

whose elements are defined by

$$ {}^0\boldsymbol{Q}_{\alpha\alpha' ij}=\Delta^{-1}\delta_{\alpha\alpha'}\delta_{ij}+2\xi K_0[\kappa R_{\alpha\alpha'}(i,j)], $$

$$ \boldsymbol{Q}_{\alpha\alpha' ij}(k)=\Delta^{-1}\delta_{\alpha\alpha'}\delta_{ij}+2\xi K_0[R_{\alpha\alpha'}(i,j)\sqrt{\kappa^2+k^2}], \tag{3} $$

respectively. Here the subscript α runs over cylinders and $R_{\alpha\alpha'}(i,j)$ is the distance between slab i on cylinder α and slab j on cylinder α'. The Manning parameter ξ is the ratio ℓ_B/b, where ℓ_B is the Bjerrum length $\ell_B=e^2/\epsilon k_B T$. Here, ϵ is the dielectric constant of the solvent. The Debye screening parameter is given by $\kappa^2=8\pi\ell_B I$ where I is the ionic strength of the solution. The parameter $\Delta=f_1/N+Z^2 f_2/N$ measures the strength of charge fluctuations per site. Finally, $K_0(x)$ is the zeroth-order modified Bessel function of the second kind. The free energy of the two parallel cylinders per unit length (measured in monomers) is then

$$ \begin{aligned} \beta\mathcal{F}_{\rm cyl}=&\frac{1}{2}q^2\sum_{\alpha=I}^{II}\sum_{ij=1}^{N}[\Delta^{-1}\delta_{\alpha\alpha'}\delta_{ij}-\Delta^{-2}\,{}^0\boldsymbol{Q}^{-1}_{\alpha\alpha' ij}] \\ &+\frac{b}{2}\int_{-\infty}^{\infty}\frac{dk}{2\pi}\ln[\det\boldsymbol{Q}(k)]+N\ln\Delta \\ &-2N\Delta\ell_B\int_{-\infty}^{\infty}K_0(b\sqrt{\kappa^2+k^2}). \end{aligned} \tag{4} $$

The first term represents the repulsion between cylinders of net charge $q=(-1+f_1+Zf_2)$ per monomer, which is screened due to the condensed counterions and free ions. The second and third terms represent counterion-mediated attractions between cylinders and the last term is the self-energy, which should be subtracted. The free energy can be evaluated numerically, given the fractions of condensed counterions and condensed cations f_1 and f_2 which determine the net charge q and the variance Δ. We solve for f_1 and f_2 self-consistently by minimizing the total free energy of the system, including the entropy of mixing of the ions and the interaction of free ions with the cylinders. To calculate this free energy, we enclose the system inside a big cylinder of radius $L_\perp$ and length $L=Mb$. This is a straightforward generalization of Eq. (5) in Ref. [5] to two cationic species, with $\mathcal{F}_{\rm cyl}$ given by Eq. (4).

Note that we have treated the counterions as point ions in this calculation. Thus, we have used the ''thermal fluctuation'' approach to describe the attraction between the cylinders. An alternate approach, the ''ionic crystal'' approach, has also been proposed to describe attractions between like-charged rods [6–9]. The discrepancy between the ionic-crystal approach and the thermal-fluctuation approach described above has led to considerable controversy [11,12]. We emphasize that there is no way to reconcile the two approaches completely, because the thermal-fluctuation approach is a high-temperature approximation, while the ionic-crystal approach is a low-temperature approximation, and the two are separated by a phase transition, namely crystallization. The thermal fluctuation approach neglects correlations that are important at low temperatures because it neglects a length scale that is important at low temperatures or high densities, namely the ionic size. This size prevents the attractive interaction from diverging and is clearly important to ionic crystallization because if all the ions were point charges, the system would collapse onto a point at zero temperature. We have shown that it is straightforward to include this length scale within a field theoretical approach by assuming that charge is correlated over the size of the ion [5]. We call this approach the charge-fluctuation approach to distinguish it from the thermal-fluctuation approach, which assumes point ions. When the nonzero ionic size is incorporated in this way, we find oscillatory charge correlations that grow in range as the temperature is lowered, and eventually diverge at the spinodal for the ionic crystal [10]. Thus, the one-loop field-theoretical approach leads to reasonable qualitative behavior at low temperatures, even though it is unlikely to be quantitatively accurate there. More recently, it has been shown for the case of two plates [13] that at high temperatures, long wavelength fluctuations in the charge density along the plates dominate the interaction, while at low temperatures, short wavelength fluctuations dominate. If the amount of counterion condensation is fixed, the long wavelength fluctuations (captured in the thermal-fluctuation approach) lead to an attraction that diminishes as temperature is lowered, while the short wavelength fluctuations (captured below the freezing transition within the ionic-crystal approach) lead to an attraction that increases as temperature is lowered. However, it is important to note that the amount of counterion condensation increases as temperature is lowered, leading to a reduction of the net charge and an increase in the attraction. This leads to a nontrivial temperature dependence of the long-wavelength attraction.

In order to establish a criterion for the validity of the thermal fluctuation approach, we must use an approach that can capture both the short and long wavelength physics-,namely, the charge-fluctuation approach. (Note that the ionic crystal approach cannot produce such a criterion, because it does not capture the attraction due to long wavelength fluctuations.) For the case of two charged surfaces separated by a distance of 5 Å, the charge-fluctuation approach leads to the criterion that the thermal-fluctuation approximation is valid when the Gouy-Chapman length $\lambda = 1/2\pi Z\sigma\ell_B$, where $1/\sigma$ is the area per surface charge, satisfies $\lambda/a > 0.035$ where a is the counterion diameter [13]. In our case, the appropriate area per surface charge is $1/\sigma = \pi D b$, where D is the cylinder diameter and b is the length of a monomer. For DNA in aqueous solution at room temperature, $b \approx 1.7$ Å and $\ell_B \approx 7.1$ Å. Thus we obtain the criterion $Z < 3.5D/a$ for the thermal-fluctuation approach to be valid.

The above criterion is a very rough guide, and should not be taken too seriously at a quantitative level. The calculation in Ref. [13] applies to the attraction between charged surfaces, not charged rods, and the difference in geometry should alter the numerical result for the criterion. In addition, the charge-fluctuation approach includes the ionic size in a certain way [5] but there are many other ways to do it that would lead to different answers because the short-wavelength physics is nonuniversal.

III. DEPENDENCE ON ROD DIAMETER

Given Eq. (4), we can examine the effect of rod diameter on the effective interaction between two cylinders. In the following figures, polyvalent counterions are divalent so $Z = 2$, the temperature is $T = 300$ K, the solvent dielectric constant is $\epsilon = 80$, the size of a site is $b = 1.7$ Å, and the total rod length is $M = 300$ monomers (this corresponds to a rod length of approximately 500 Å, which is the persistence length of DNA). The counterion diameter is assumed to be $a = 4.2$ Å. The ionic strength of the solution is taken to be 50 mM (characteristic of conditions for DNA condensation) and $L_\perp = L \approx 500$ Å.

Before presenting our results, we must discuss whether the thermal-fluctuation approach that we have used is valid. In the discussion at the end of Sec. II, we showed that the approach is valid as long as $Z < 3.5D/a$. For a counterion valence of $Z = 2$ and counterion diameter of $a = 4.2$ Å, this implies that the approach is valid for $D > 2$ Å.

In Fig. 1, we plot the free energy $F_{\rm cyl} = M\mathcal{F}_{\rm cyl}$ as a function of the surface-to-surface separation r between the two cylinders. The zero of free energy is chosen to correspond to $r = \infty$. Each curve corresponds to a different value of the cylinder diameter D, ranging through the values $D = 0$, 10.9, 16.3, 21.7, and 27.1 Å from the innermost curve (dotted) to the outermost one. The case of DNA corresponds approximately to the second-to-last curve. The effect of the nonzero rod diameter is striking. As the diameter increases, the free energy develops a pronounced barrier, of height $F_{\rm barrier}$.

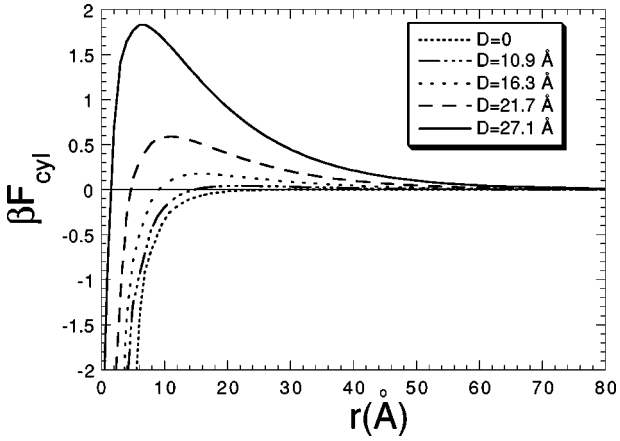

FIG. 1. Free energy of interaction between two cylinders, $F_{\rm cyl}$, as a function of the surface-to-surface separation r for different rod diameters D. The parameters are $T = 300$ K, $\epsilon = 80$, and $Z = 2$ (divalent counterions). The main effects of increasing the rod diameter are to increase the repulsive barrier and to shift the attraction to smaller separations.

We have no short-ranged repulsion because we have neglected hardcore interactions, so the free energy diverges to $-\infty$ as the rod separation r decreases. As a result, we cannot examine trends in the attractive part of the free energy by measuring the free energy minimum. However, we can study the change in the attractive part of the free energy by measuring the free energy at an arbitrary, but short, separation. We have chosen to measure the free energy at a surface-surface separation of $r = 6$ Å; we call this $F_{\rm att}$. The main reason for choosing $r = 6$ Å, rather than some other length, is that this is approximately the surface-to-surface spacing of condensed DNA chains in a bundle [2]. In Fig. 2 we have plotted the $F_{\rm att}$ (solid line), as well as $F_{\rm barrier}$ (dotted line), as a function of D. Figure 2 shows that $F_{\rm att}$ becomes less nega-

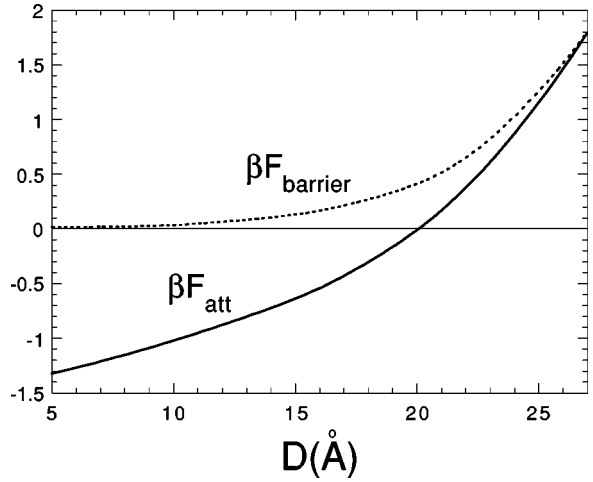

FIG. 2. Free energy at $r = 6$ Å (approximately the separation of chains in a condensed DNA bundle), $F_{\rm att}$, and barrier height, $F_{\rm barrier}$, as functions of the rod diameter D. We have chosen $T = 300$ K, $\epsilon = 80$, and $Z = 2$. Both $F_{\rm att}$ and $F_{\rm barrier}$ increase with increasing D. In particular, note that the attraction disappears for sufficiently large D.

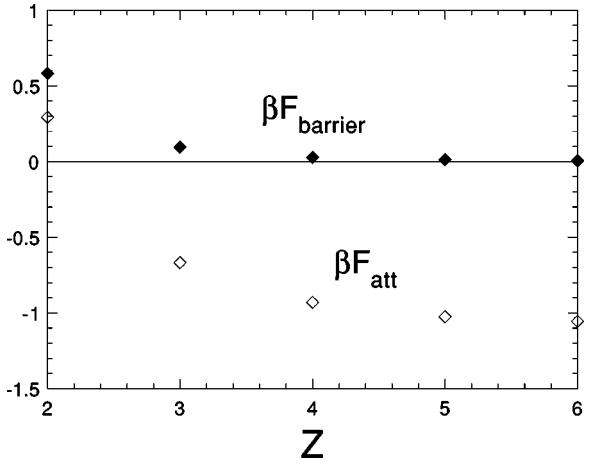

FIG. 3. Free energy at $r=6$ Å, F_{att} (filled diamonds), and barrier height F_{barrier} (open diamonds), as functions of the counterion valency Z for $T=300$ K, $\epsilon=80$, and $D=21.7$ Å (approximately the diameter of double-stranded DNA; our model only allows values of D quantized in units of the monomer length b). Both quantities decrease with increasing Z, but beyond $Z=3$, both quantities are roughly independent of Z. Note that counterions with $Z\geqslant 3$ are required for two cylinders of this diameter to attract each other at a surface-to-surface spacing of $r=6$ Å.

tive as D increases, implying that the attraction grows weaker. The dotted line shows that F_{barrier} becomes more positive as D increases, also implying that the attraction grows weaker relative to the repulsion. These trends can be understood by considering the nature of counterion-mediated interaction. Since the attraction is very short-ranged and depends very sensitively on separation, a smaller fraction of the surface of each cylinder is involved in the attraction as the cylinder diameter increases. On the other hand, the total number of condensed counterions remains roughly constant as the diameter increases, so the net charge (which controls the repulsive interaction between the rods) remains about the same. As a result, the attraction is diminished relative to the repulsion as the diameter increases.

Note that the curves in Fig. 2 were calculated for the case where the multivalent counterions are divalent, $Z=2$. For this case, we find that the attraction disappears, that is, F_{att} changes sign, at $D\approx 20$ Å. This is approximately the diameter of double-stranded DNA. Thus, divalent ions are marginal for DNA condensation within our model. This is in good agreement with experimental results [2].

IV. DEPENDENCE ON COUNTERION VALENCY

We have also examined the dependence of the barrier height F_{barrier} and the free energy at $r=6$ Å, F_{att}, on the counterion valency Z. Here we have chosen a cylinder diameter of $D=21.7$ Å, close to that of DNA. (The actual diameter of double-stranded DNA is 20 Å, but our model requires $D=Nb$, where N is an integer and b is the monomer length. As a result, our values of D are quantized in units of the monomer length.) For this value of D, the approximations we have adopted should be valid for $Z<17$. As shown in Fig. 3, both F_{barrier} and F_{att} decrease with the increasing valency Z. This implies that the attraction grows stronger relative to the repulsion with increasing counterion valency. The reason for this is twofold. First, the net charge on each macroion decreases with Z (there is more counterion condensation as the counterion valency increases). This weakens the repulsive interaction due to the net charge. Second, the strength of the charge fluctuations grows with increasing Z (i.e., $N\Delta=f_1+Z^2f_2$ where $f_2\sim 1/Z$). This strengthens the correlation attraction between the chains. Most of the condensed counterions are multivalent because there is a greater energetic gain for condensation for the same entropic cost for multivalent counterions as compared to monovalent ones.

Note that F_{att} is negative only for $Z\geqslant 3$. Since $r=6$ Å is a typical spacing of DNA in a condensed bundle, this implies that a counterion valence of $Z\geqslant 3$ is required in order for the chains to condense. This is consistent with experimental findings [2].

Interestingly, Fig. 3 also shows that both F_{barrier} and F_{att} become nearly independent of valency for $Z\geqslant 3$. This is also consistent with experimental findings [2] that the characteristics of condensed DNA bundles appear to be independent of counterion valency for $Z\geqslant 3$. The reason for this puzzling behavior can be understood quite simply. Although *condensed* counterions of higher valency induce stronger attractions, *free* counterions of higher valency screen electrostatic interactions more efficiently. These two effects tend to cancel each other out, leading to a nearly flat dependence of the free energy on Z for sufficiently high Z.

V. SUMMARY

In previous papers, we assumed that the charge on a rod, and the charge fluctuations resulting from counterion density fluctuations along the length of the rod, are positioned along the center axis. Here, we have generalized our approach to allow for two-dimensional charge fluctuations on the surface of a cylindrical rod with nonzero diameter. The resulting balance between attractive and repulsion interactions between two rods is significantly altered. In particular, we find that for sufficiently thick rods, there is no attraction at all. If we denote the diameter at which the attraction disappears as D_{max}, we find that D_{max} increases with increasing counterion valency, and that D_{max} increases with decreasing rod separation r in a bundle.

One puzzling experimental observation has been that the nature of DNA bundles (i.e., the spacing of chains in a bundle and the size of bundles) appears nearly independent of the bundling agent as long as the valency satisfies $Z\geqslant 3$. This is surprising for an effect that is believed to be mostly electrostatic in origin. Here, we have shown that increasing the counterion valency has relatively little effect for $Z\geqslant 3$. This remarkable result occurs because the increased valency leads to stronger screening as well as stronger attractions. Thus, our model of DNA condensation appears consistent with the known facts.

ACKNOWLEDGMENTS

We gratefully acknowledge the support of the National Science Foundation through Grant No. DMR-9619277.

[1] J.L. Barrat and J.F. Joanny, Adv. Chem. Phys. **94**, 1 (1996).
[2] V.A. Bloomfield, Biopolymers **31**, 1471 (1991); **44**, 269 (1997).
[3] A.W. Lau and P. Pincus, Phys. Rev. Lett. **81**, 1338 (1998).
[4] A.A. Korynshev and S. Leikin, J. Chem. Phys. **107**, 3656 (1997); Biophys. J. **75**, 2513 (1998).
[5] B.-Y. Ha and A.J. Liu, Phys. Rev. E **60**, 803 (1999).
[6] I. Rouzina and V.A. Bloomfield, J. Phys. Chem. **100**, 9977 (1996).
[7] N. Grønbech-Jensen, R.J. Mashl, R.F. Bruinsma, and W.M. Gelbart, Phys. Rev. Lett. **78**, 2477 (1997).
[8] B.I. Shklovskii, Phys. Rev. Lett. **82**, 3268 (1999).
[9] J.J. Arenzon, J.F. Stilck, and Y. Levin, Eur. Phys. J. B **12**, 79 (1999).
[10] B.-Y. Ha and A.J. Liu, Phys. Rev. E **58**, 6281 (1998).
[11] Y. Levin, J.J. Arenzon, and J.F. Stilck, Phys. Rev. Lett. **83**, 2680 (1999).
[12] B.-Y. Ha and A.J. Liu, Phys. Rev. Lett. **83**, 2681 (1999).
[13] B.-Y. Ha (unpublished).